Electromagnetic Metasurfaces and Reconfigurable Metasurfaces: A Review

Sidrish Zahra, Liang Ma, Wenjiao Wang, Jian Li*, Dexu Chen, Yifeng Liu, Yuedan Zhou, Na Li, Yongjun Huang* and Guangjun Wen

School of Information and Communication Engineering/Sichuan Provincial Engineering Research Center of Communication Technology for Intelligent IoT, University of Electronic Science and Technology of China, Chengdu, China

Metamaterial is a kind of material/structure that is artificially designed and has exceptional electromagnetic properties and/or other physical properties, not found in nature. A class of electromagnetic metamaterial with only one or a few layers of periodic or aperiodic arranged cell structures in the direction of electromagnetic waves propagation can be referred to as a metasurface. Metasurface can be considered as a two-dimensional representation of metamaterial and can realize the controlling of the amplitude, phase, and polarization state/direction of the incident electromagnetic wave. According to the novel electromagnetic characteristics of metasurface and its big advantages, a series of new planar devices and systems based on metasurface can be developed. The goal of this review article is firstly to provide introductions for basic metasurface, its significance properties, and application principles. Meanwhile, the main research progresses of regular metasurfaces and the newly developed reconfigurable metasurfaces are analyzed, focusing on the types of amplitude modulation, phase modulation, polarization modulation, and multidimensional modulation. Finally, the research significances of metasurface development trend and important engineering practical applications are analyzed in the end.

Keywords: metamaterial, metasurface, reconfigurable, wave-front manipulation, applications

INTRODUCTION

Metamaterial is a kind of synthetic structural *material* with singular electromagnetic, acoustic, or mechanical characteristics [1–6]. One can select the appropriate substrate types according to different application requirements and design subwavelength-scale structure (meta-atom) with different shapes, sizes, and rotation directions. According to the subwavelength period or nonperiodic array arrangements, the designed metamaterial can control independently/coherently the amplitude, phase, polarization state/direction, and other parameters of the incident electromagnetic/acoustic wave as needed. In correspondence to this, novel planar functional devices and systems working in different frequency bands such as low frequency, high frequency, microwave, THz, and visible light can be developed [7–16]. Therefore, metamaterials have important application prospects in the fields of science and engineering such as acoustics/mechanics, electromagnetics, optics, and thermodynamics. A class of *electromagnetic* metamaterial consisting of only one layer or a few layers of periodic or aperiodic elements in the direction of electromagnetic wave propagation is also called electromagnetic metasurface [17–21]. The electromagnetic metasurface has subwavelength thickness in the direction of electromagnetic

wave propagation, small size, and light weight, but it can realize the similar electromagnetic wave characteristic controlling abilities as the classical three-dimensional electromagnetic metamaterial. In recent years, therefore, the research on metasurface has become one of the hotspots in the academic and industry areas [22–35].

Based on the Huygens' principle, each subwavelength structure unit of the electromagnetic metasurface will generate a spherical wave packet at the metasurface-air interface under the action of incident electromagnetic waves. The spherical wave packets generated by all metasurface units form a new electromagnetic wave-fronts [36]. Therefore, each metasurface unit can be reversely designed according to the required electromagnetic wave-fronts. And accordingly the electromagnetic wave-fronts can be controlled by adjusting the shape, size, and direction of the metasurface unit [36–40]. Different from conventional large-scale planar optical components or microwave phased array antennas, the metasurface can control and adjust the characteristics of near-field electromagnetic wave in the subwavelength range. It is possible to develop several new high-performance thin-film, ultraminiature planar electromagnetic or optical devices including spatial filters [41, 42], focusing lens [43, 44], beam polarization deflection/converters [45, 46], special beam shaping devices [47, 48], and holographic imaging plates [49, 50]. Therefore, it is of great scientific value to explore and develop a new mechanism, new method, and process technology of artificially synthesized electromagnetic metasurface in the advanced electromagnetic community. In the past decade, many good review articles have been published to summarize the developments of metasurfaces [40, 51–60]. However, those review articles only focused on some parts of the research aspects, like the fundamentals and the specific applications. Most importantly, only a few review articles summarized the research developments of the basic metasurfaces and the tunable/reconfigurable metasurfaces. In this review, therefore, we would like to summarize the recently developed different kinds of electromagnetic metasurfaces and reconfigurable electromagnetic metasurfaces and devise some new research directions.

Research Progress on Basic Metasurfaces

The main technical realization ways of synthetizing metasurface can be divided into plasmonic-like structure based on metallic materials [36, 37], full dielectric photonic structure based on high refractive index materials [33, 38–40], and other novel structures based on novel thin film materials, semiconductor materials, quantum dots, etc. [33, 36–40, 61, 62]. Most of the reported metasurfaces are used to realize the manipulations of the amplitude, phase, and polarization together with other parameters of the incident electromagnetic waves.
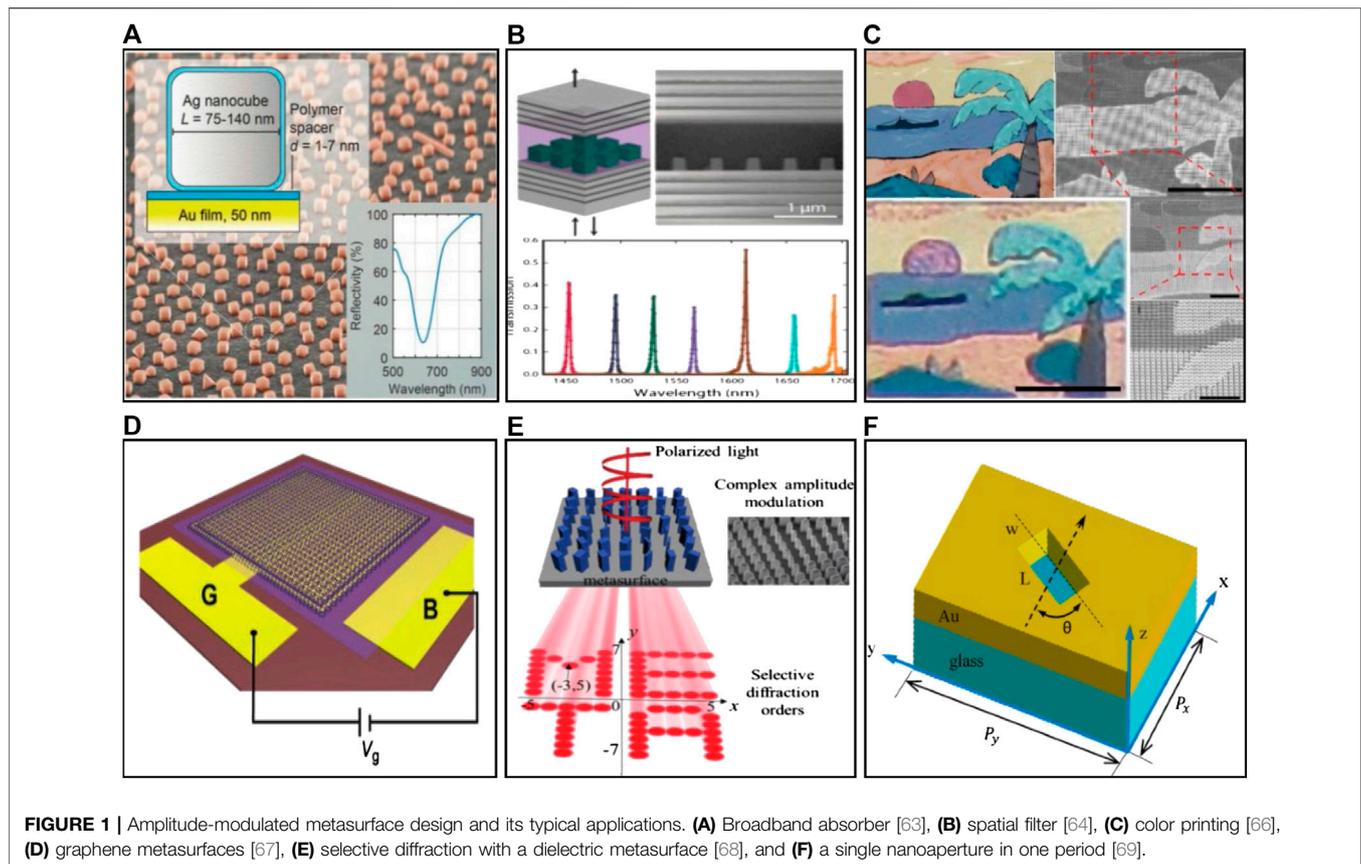
Metasurface for Amplitude Modulation

The metasurface that realizes the amplitude control of electromagnetic waves is mainly used to reflect, absorb, or transmit the incident electromagnetic wave energy. In recent years, a large number of related results have been reported, such

as the broadband metasurface absorber [12–15, 63], metasurface space filter [64, 65], metasurface color printing [66], graphene metasurface anomalous refraction plate [67], dielectric metasurface for selective diffraction [68], and metasurface for near-field plasmonic beam engineering [69], as concluded in **Figure 1**.

Specifically, the representative broadband metasurface absorber shown in **Figure 1A** is fabricated on a flexible substrate by using the nanoscale metal particles arranged in a nonperiodic manner so that the entire metasurface can be conformally mounted on a nonplanar carrier [63]. When the metal particles resonate, the equivalent impedance of the entire metasurface is matched with the free-space wave impedance. The high dielectric loss and magnetic loss generated by the resonance absorb the incident electromagnetic wave energy and the square metal particles have polarization insensitive ability. Thereby the entire metasurface absorber can achieve high-performance absorptions in the near-infrared band and wide angle of incidence. The structure in **Figure 1B** consists of a layer of dielectric metasurface and two layers of distributed Bragg reflectors which can be integrated into various planar optical components [64]. The upper and lower distributed Bragg reflectors form a typical Fabry–Pérot resonator. The metasurface of the middle layer realizes the control of the resonance frequency and constitutes a high-performance (high frequency-selectivity) space electromagnetic wave signal filter. The metasurface in **Figure 1C** consists of a metal plasmonic cell that reproduces the color pattern captured by the camera [66]. Each metal unit resonates with different electromagnetic wave reflection coefficients in the visible frequency region so the human eye can observe different colors. Based on this characteristic, the original color pattern can be reproduced by designing the corresponding metal unit and array, according to the color information of each pixel in the previously taken color photograph.

Moreover, as can be seen in **Figure 1D**, an active metasurface can be formed by integrating graphene into a U-shaped aperture size via a single layer configuration [67]. The hybrid graphene metasurface composed of the artificially constructed two-dimensional metal hole array at the subwavelength scale and the naturally occurring graphene constitutes an electrically steerable amplitude anomalous refraction. Based on the Pancharatnam–Berry phase and the suitable spatially linear phase differences, the amplitude modulation for circularly polarized terahertz wave with anomalous refraction can also be achieved by the effective modulation of the gate voltage. Advanced applications for the dynamic control of electromagnetic waves by electrically tunable graphene metasurfaces such as amplitude tunable active focusing lenses are proposed [67]. More research progress for the dynamic controllable metasurfaces will be discussed in details in the next section. In **Figure 1E**, a complex amplitude modulation based on the ultrathin dielectric metasurface is used to create a new method for independently selecting diffraction orders based on the adjustment of the geometric parameters of the custom nanostructures [68]. **Figure 1F** also shows a near-field plasma beam engineering of metasurface using nanoaperture

FIGURE 1 | Amplitude-modulated metasurface design and its typical applications. **(A)** Broadband absorber [63], **(B)** spatial filter [64], **(C)** color printing [66], **(D)** graphene metasurfaces [67], **(E)** selective diffraction with a dielectric metasurface [68], and **(F)** a single nanoaperture in one period [69].

arrays to effectively control the complex amplitude of the surface plasmon polaritons in the near-field region [69]. In such a design, each individual nanoaperture is determined pixel by pixel. As a result, the amplitude can be determined by the different lengths of the nanoaperture and the complex amplitude modulation of the surface plasmon polaritons is realized.

Those metasurfaces mentioned above are designed according to the specific application requirements. Each metasurface unit is arranged in a periodic or aperiodic manner to realize the control of the amplitude of the electromagnetic wave. However, when such metasurfaces are designed and developed, their electromagnetic wave amplitude control characteristics are fixed and cannot be changed.
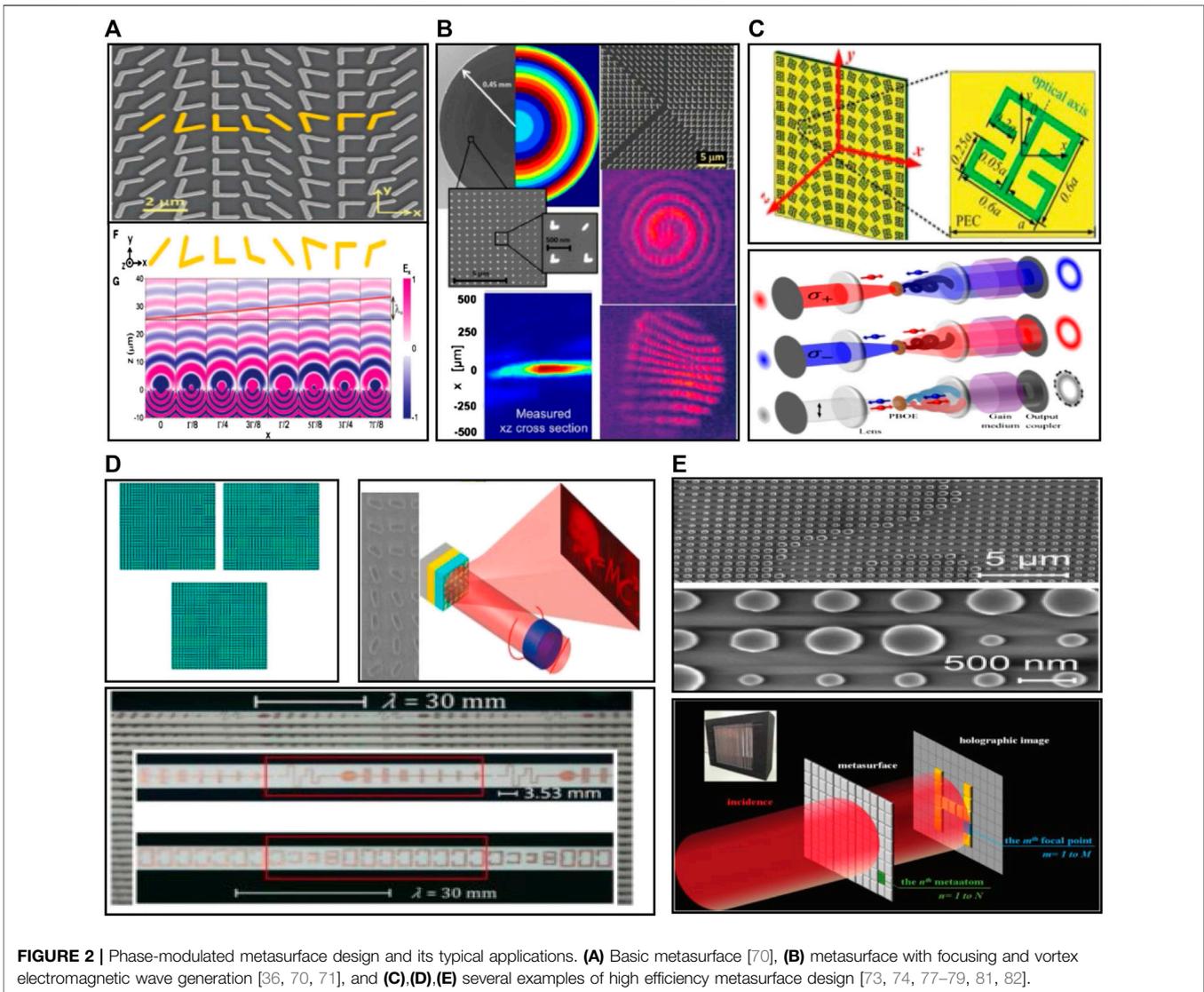
Metasurface for Phase Modulation

On the other hand, the phase response characteristics of metasurface are also closely related to the size, shape, rotation mode, and the substrate material type of the metasurface unit. Therefore, each metasurface unit can be reversely optimized as well as designed according to the specific phase distribution requirements to achieve the phase control of the electromagnetic wave. As early as 2011, N. Yu et al. used eight metasurface elements of different shapes to effectively achieve phase manipulation in the range of 0-2π based on the principle as shown in **Figure 2A** [70]. And a metasurface having flat focusing function and vortex electromagnetic wave generating function

based on the phase manipulation has been developed as can be seen in **Figure 2B** [36, 70, 71].

The phase-modulated metasurface initially reported controls only the crosspolarization component of the incident electromagnetic wave, but most of the common polarization components of the incident electromagnetic wave are not effectively utilized. As a consequence, its electromagnetic wave conversion efficiency is extremely low [62, 72]. To solve this problem, researchers have proposed several kinds of new structures such as Pancharatnam-Berry (P-B) phase metasurface, reflective-type metasurface, Huygens' metasurface, double-layer and multilayer metasurface to realize high-efficient electromagnetic wave manipulation.

P-B phase metasurface. The P-B phase metasurface is a type of structure that can continuously control the phase of electromagnetic waves by changing the rotation angle of the metasurface unit. In 2015, X. Ding et al. designed the P-B phase metasurface structure as shown in the first subplot in **Figure 2C**, and a high-performance flat-focus lens has been developed which achieves nearly 25% electromagnetic wave control efficiency [73]. The same year D. Wen et al. designed a high-efficient holographic imaging plate based on another P-B phase metasurface structure [74], as shown in the second subplot of **Figure 2C**. Moreover, based on the geometric P-B phase, the intracavity laser mode is controlled topologically to achieve a high modulus purity of ~95% [75]. Following the transmissive ultrathin P-B metasurfaces, the photonic spin Hall (PHSE)

FIGURE 2 | Phase-modulated metasurface design and its typical applications. **(A)** Basic metasurface [70], **(B)** metasurface with focusing and vortex electromagnetic wave generation [36, 70, 71], and **(C)**,**(D)**,**(E)** several examples of high efficiency metasurface design [73, 74, 77–79, 81, 82].
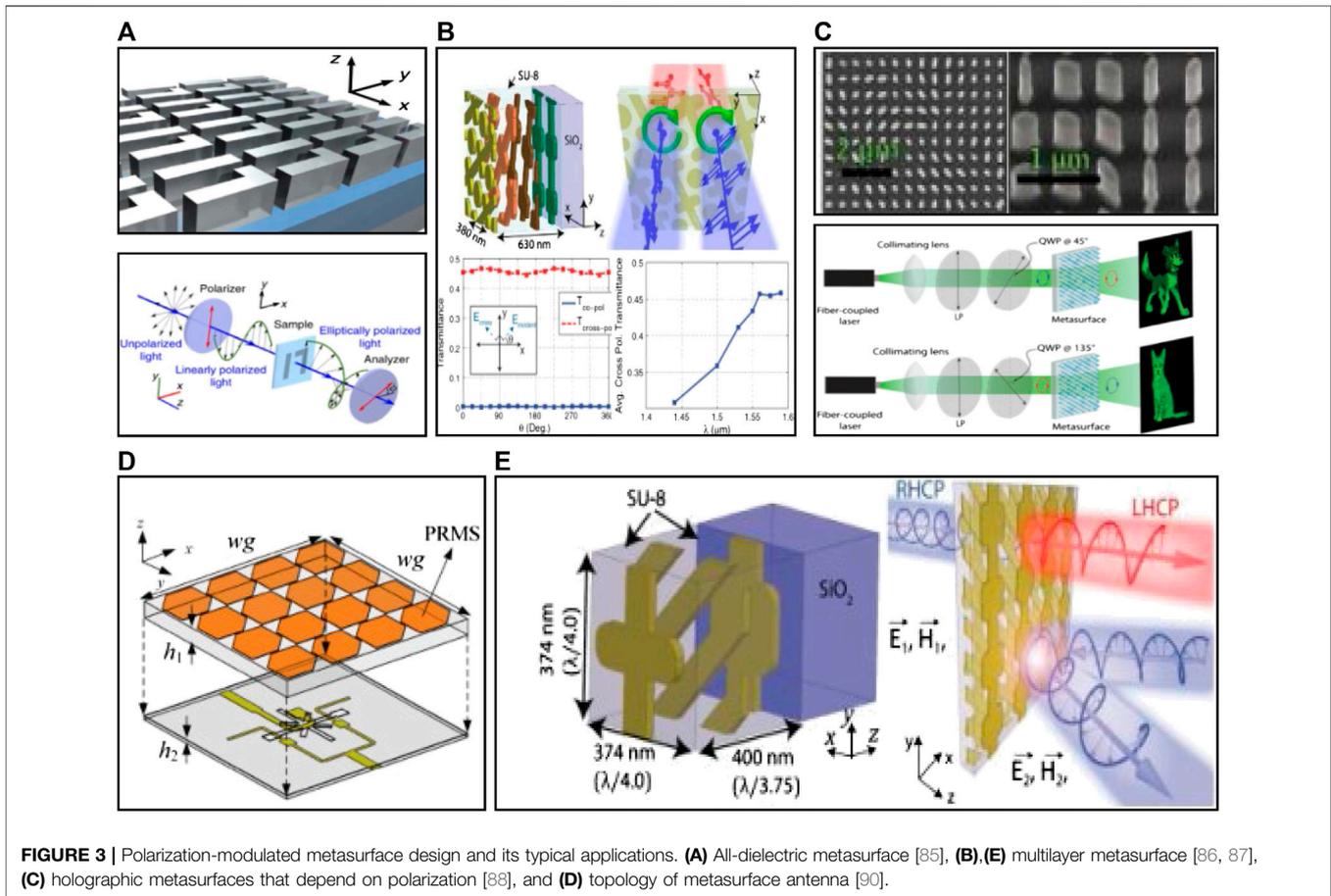
effect can be observed and the efficiency is close to 100%. At the same time, the microwave metasurface with a three-layer structure (total thickness still much smaller than the operating wavelength) is designed (the maximum PSHE efficiency can reach up to 91%), stimulating other P-B metadevices with high efficiency and high performance [76].

Reflective-type metasurface. Moreover, the magnetic resonance characteristics can be formed between the metasurface unit and the metal back-plate in the reflective-type metasurface structures so that the control efficiency of incident electromagnetic waves can be greatly improved. Based on the previously reported P-B phase, a reflective-type P-B phase metasurface with different phases is used combined with different predesigned coding sequences to control the terahertz wave. The coded P-B phase metasurface provides the ability to reduce broadband radar cross section and proposes a flexible way to manipulate reflected terahertz waves [77] as shown in the first subplot of **Figure 2D**. In 2015, G. Zheng et al. designed an

I-shaped reflective-type metasurface holographic imaging plate as can be seen in the second subplot of **Figure 2D**, which realized phase control of incident electromagnetic waves with its control efficiency reaching up to 80% [78].

Huygens' metasurface. Based on the Huygens' principle, the Huygens' metasurface which can produce both electric and magnetic resonance was designed to control the electric and magnetic field components of the incident electromagnetic wave. As a result, it has a nearly nonreflecting and completely matching transmission characteristics to maximize the control efficiency of the electromagnetic wave. In 2013, within this frame, C. Pfeiffer et al. designed and developed a Huygens' metasurface with electromagnetic wave control efficiency up to 86% in microwave frequency band [79], as shown in the last subpicture of **Figure 2D**. They also realized the transmission direction control of electromagnetic beam and the Gauss-Bessel beam conversion. Subsequently, C. Pfeiffer et al. further developed a Huygens' metasurface in the near infrared band

FIGURE 3 | Polarization-modulated metasurface design and its typical applications. **(A)** All-dielectric metasurface [85], **(B),(E)** multilayer metasurface [86, 87], **(C)** holographic metasurfaces that depend on polarization [88], and **(D)** topology of metasurface antenna [90].

[80]. In 2016, L. Wang et al. designed a grayscale metahologram as can be seen in the first subpicture of **Figure 2E**, based on the Huygens' principle. They realized phase control and its control efficiency is up to 99% [81]. In 2018, following the developments of Huygens' metasurface with complete phase shift coverage, Z. Wang et al. proposed a novel Huygens' metasurface hologram at microwave frequency, with detailed studies for the electromagnetic field distribution at the control interface and the energy distribution between the modulation focal points and microwave imaging. This proposed Huygens' metasurface extends the approach of holographic microwave applications [82] as shown in the last subpicture of **Figure 2E**.

In recent years, researchers have also proposed double-layer and multilayer metasurface designs, for further improving the efficiency of controlling the phase of electromagnetic waves. A variety of flat functional devices are reported, e.g., in [83, 84].

As can be seen above, a variety of novel planar devices with beam focusing, transmission direction control, vortex electromagnetic wave generation, holographic imaging, and other functions have been developed using phase-modulated metasurfaces. It is the most well-developed metasurface research areas in recent years. However, the phase-modulated metasurfaces and the realized electromagnetic wave control characteristics based on the planar functional devices have also been defined to be incapable of real-time dynamic tuning.

Metasurface for Polarization Modulation

By designing an asymmetric metasurface unit, the phase difference of the transmitted or reflected electromagnetic waves in the orthogonal direction can be realized. As a result, the control of the polarization direction of the electromagnetic wave and the conversion between various polarization states of the electromagnetic wave were achieved [62, 72]. For example, in 2014, C. Wu et al. developed an all-dielectric metasurface as shown in **Figure 3A** which has Fano's asymmetric resonance characteristics. It can convert linear polarization wave into circular polarization wave radiation [85]. In the same year, C. Pfeiffer et al. developed a multilayer metasurface unit structure as can be seen in **Figure 3B** which can realize the asymmetric transmission of circularly polarized waves and achieve the reversal of polarization states [86]. In 2016, C. Pfeiffer et al. continued to develop a multilayer metasurface structure as shown in **Figure 3E** which can realize the control of the polarization direction of linear polarization waves [87]. In 2017, based on this type of metasurface, J. Mueller et al. designed a holographic metasurface that exhibits different response characteristics for different polarized electromagnetic wave excitations [88] as directed in **Figure 3C**. In the same year, based on the anisotropic metasurfaces, X. Huang et al. achieved the polarization of circularly polarized waves with high conversion efficiency over a wide frequency range [89]. In 2018, W. Yang

et al. proposed a low-profile broadband double-circularly polarized metasurface antenna and thus it can be extended to construct a 2 × 2 dual circularly polarized antenna array [90] as shown in **Figure 3D**. The working state of the above-reported metasurface, however, also fails to achieve on-demand real-time dynamic tuning.

Metasurface for Multidimensional Modulation

All the above-mentioned metasurfaces are only able to control one single degree of freedom, e.g., amplitude, phase, or polarization of incident electromagnetic waves. In order to achieve more precise control of electromagnetic waves for high-performance holographic imaging and special beam generation, it is necessary to simultaneously control the amplitude and phase (or phase and polarization) of incident electromagnetic waves. For examples, in 2014, L. Liu et al. proposed a combination of amplitude-modulated metasurface units with phase-modulated metasurface units to achieve simultaneous control of amplitude and phase of electromagnetic wave and also developed a broadband metasurface in the THz band [91]. Subsequently, Z. Li et al. designed and developed the nondiffracting beam radiation metasurface in the near-infrared frequency band [92, 93] based on I-shaped metasurface units and C-shaped metasurface units for simultaneous control of electromagnetic wave amplitude and phase. In 2018, G. Lee et al. proposed a new metasurface consisting of X-shaped meta-atoms to achieve full complex amplitude and phase modulation in the broadband visible wavelength region. It was almost comparable to an ideal 3D hologram, and the beam shaping, 3D bioimaging, optical computing, and optical chips can be developed based on such kind of metasurface [94].

Furthermore, in 2015, J. Li et al. proposed a metasurface unit with different rectangular channels which can control simultaneously the polarization and phase of electromagnetic waves so that the circularly polarized incident electromagnetic waves can be converted to linearly polarized waves after passing through such metasurfaces and can deflect the transmission direction of the linear polarized wave [95]. In the same year, A. Arbabi et al. proposed an elliptical all-dielectric metasurface unit structure by designing the ellipticity and with different rotation angles of the metasurface unit. Moreover, they adopted the honeycomb periodic arrangement to realize precise control of the phase and polarization of electromagnetic waves. Based on this metasurface configuration, a variety of high-performance planar functional devices with electromagnetic wave utilization efficiency of up to 97% have been developed, which can realize polarization separation and focusing, polarization transformation and focusing, holographic imaging, and vortex electromagnetic wave generation functions [61].

In 2018, Y. Zhou et al. used lattice design and different arrangements to achieve multifunction reconfigurable metasurface based on amplitude, phase, and polarization modulation fully reflecting the control ability of
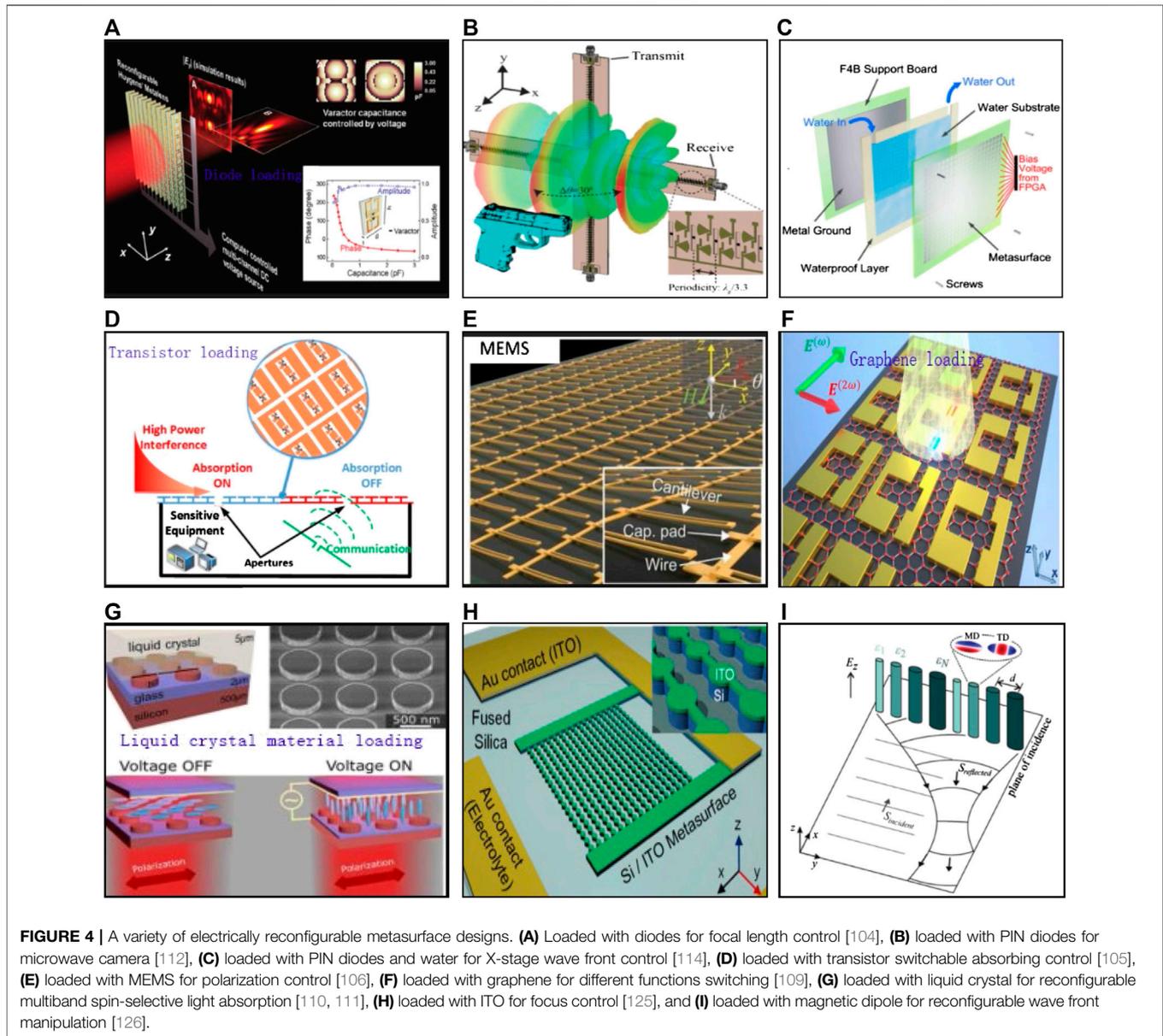
electromagnetic wave [96]. At the same time, H. Xu et al. developed a multilayer C-shaped chiral metasurface structure, which was able to control the amplitude, phase, and polarization parameters of electromagnetic waves independently, and proposed several functional flat structures, such as dual focus prisms, airy beams, and multibeam shaping [97]. However, these metasurfaces with multidimensional parameters control ability still cannot achieve real-time dynamic control of incident electromagnetic waves.

Research Progress on Reconfigurable Metasurfaces

The above-reported metasurfaces can control the amplitude, phase, polarization, and other parameters of the electromagnetic wave as needed, and, therefore, it can develop various planar functional devices with novel functions at different frequency regions. However, when those metasurfaces are designed and fabricated, their specific electromagnetic wave characteristic control abilities are limited and cannot be changed, as concluded in previous section. In recent years, in order to achieve higher degree-of-freedom electromagnetic wave control and utilization, active tunable/reconfigurable/ programmable metasurfaces, nonlinear metasurface concepts and design techniques have been proposed [62, 98–103]. As mentioned in the beginning of this review, the electromagnetic response characteristics of the metasurfaces are closely related to the size, shape, rotation direction, and substrate material type of the metasurface unit. As a consequence, the electromagnetic response characteristics of the metasurface can be dynamically controlled by additionally adjusting the metasurface unit structure and the substrate material properties. In turn, the modulations of electromagnetic waves are controlled in real time, that means achieving active tunable, reconfigurable, programmable, and other versatile metasurfaces and versatile optoelectronic devices and systems based on such metasurfaces. The active tunable/reconfigurable metasurface structures that have been reported in recent years include electronic control, light control, temperature control, mechanical control, and power control, which will be discussed in detail in following parts.
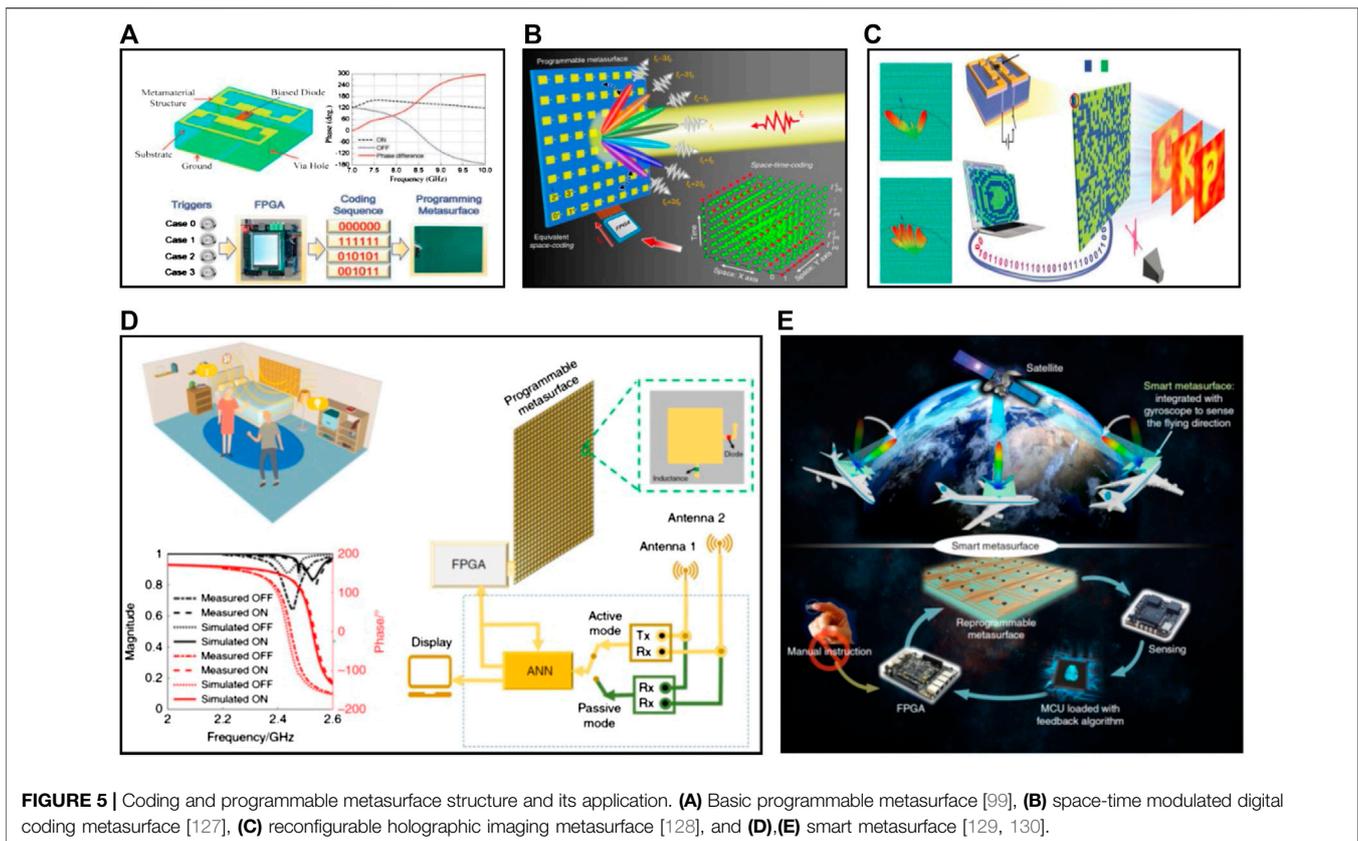
Electrically Reconfigurable Metasurfaces

For the tunable metasurfaces loaded by diodes [104], transistors [105], MEMS [106–108], graphene [109], and liquid crystals [110, 111], etc., the electromagnetic response characteristics can be dynamically controlled by adjusting the applied bias voltage on the materials/components in those metasurfaces. For examples, in 2017, K. Chen et al. achieved the electromagnetic response characteristic tuning by biasing voltage on each cell in the reconfigurable metasurface array loaded by the independent/ joint control diodes. Furthermore, the on-demand controlling of the metasurface to the incident electromagnetic wave front was realized and the adjustable focal length was developed [104] as shown in **Figure 4A**. In 2018, O. Yurduseven et al. utilized a PIN diode to dynamically tune the "ON" and "OFF" transition states of a slot-type subwavelength metamaterial unit. The waveguide mode was converted to free-space radiation using a binary

FIGURE 4 | A variety of electrically reconfigurable metasurface designs. **(A)** Loaded with diodes for focal length control [104], **(B)** loaded with PIN diodes for microwave camera [112], **(C)** loaded with PIN diodes and water for X-stage wave front control [114], **(D)** loaded with transistor switchable absorbing control [105], **(E)** loaded with MEMS for polarization control [106], **(F)** loaded with graphene for different functions switching [109], **(G)** loaded with liquid crystal for reconfigurable multiband spin-selective light absorption [110, 111], **(H)** loaded with ITO for focus control [125], and **(I)** loaded with magnetic dipole for reconfigurable wave front manipulation [126].

adjustment to form a target radiation pattern. Then a dynamically reconfigurable holographic metasurface aperture that allows for electron beam steering purposes was designed. And a synthetic K-band Mills-Cross monochrome microwave camera can be set up to achieve high fidelity images [112], seen in **Figure 4B**. In 2018, X. Gao et al. proposed an active metasurface composed of a butterfly-shaped unit cells embedded with the voltage-controlled varactor diodes. The reconfigurable polarization converter was dynamically converted from linear to linear, linear to elliptical, and linear to circular by adjusting the bias voltage of the varactor [113]. In 2019, L. Chen et al. proposed a reconfigurable metasurface using the voltage control of the PIN diode and the control of the salinity of the water matrix so that the metasurface can flexibly control the amplitude and deflection angle of the scattered beam. In turn, the X-stage wave front of the

reconfigurable water-based metasurface was controlled [114], as shown in **Figure 4C**. Moreover, in 2017, A. Li et al. developed a broadband absorbing material with adjustable switch control and absorbing power by loading transistors in the absorbing metasurface unit and adjusting the bias voltage applied to each transistor [105], as shown in **Figure 4D**.

Moreover, in 2018, X. Zhao et al first designed a MEMS-loaded reconfigurable metasurface as can be seen in **Figure 4E** by controlling the resonant characteristics of the metasurface unit through adjusting the magnitude of the bias voltage, thereby, achieving the control of the polarization state of the incident electromagnetic wave [106]. E. Arbabi et al. prepared a metasurface lens on the MEMS cantilever and controlled the position of the transmitted electromagnetic wave focus by adjusting the bias voltage [107], and, at the same time,

FIGURE 5 | Coding and programmable metasurface structure and its application. **(A)** Basic programmable metasurface [99], **(B)** space-time modulated digital coding metasurface [127], **(C)** reconfigurable holographic imaging metasurface [128], and **(D),(E)** smart metasurface [129, 130].
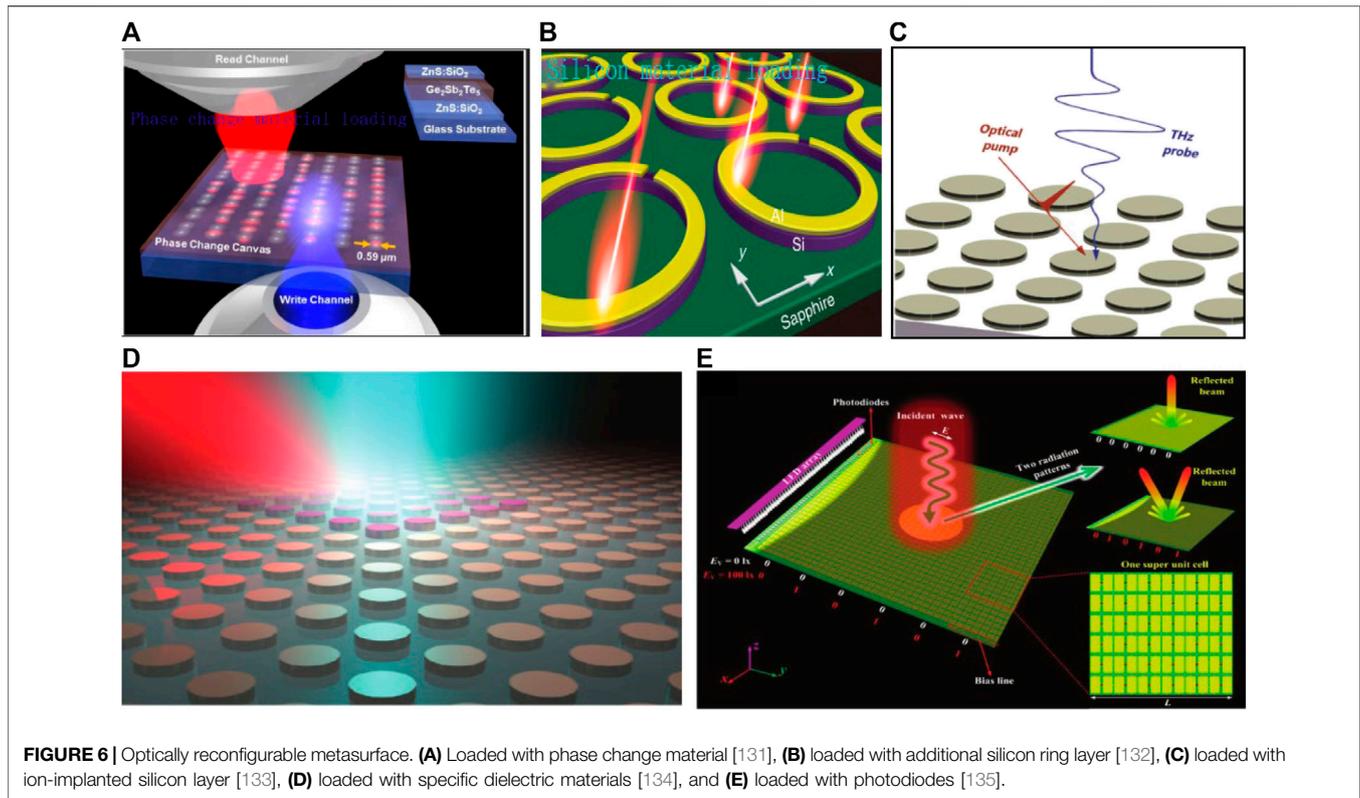
M. Manjappa et al. realized a simple logic signal processing in the THz band based on the MEMS-loaded dual SRR metasurface structure [108].

In addition, S. R. Biswas et al. theoretically proved that when the graphene material was loaded into the reflective metasurface, by changing the bias voltage of the graphene, the on-demand switching between the beam orientation/focus and electromagnetic cloak can be realized [109], seen in **Figure 4F**. As a result, the tunable frequency and/or amplitude modulation can be achieved [115, 116]. After that, many high-performance graphene-based tunable/reconfigurable metasurfaces are reported with different kinds of functions, including the tunable polarization switching/converting and beam steering [117, 118], broadband and tunable perfect absorber [119–122], and even programmable metasurface [123, 124] which will be discussed later. Moreover, A. Komar et al. and D. Xiao et al. have proposed the designs for integrating liquid crystals into metasurface arrays. By adjusting the bias voltage applied to the liquid crystals, the controlling of the metasurface resonance frequency as well as the on-demand selective absorption of electromagnetic waves of different polarizations was achieved [110, 111], as shown in **Figure 4G**. A. Howes et al. loaded the ITO material layer in the metasurface array and realized the electromagnetic wave transmittance controlling by adjusting the bias voltage on the ITO material. Finally they realized the reconfigurable focus beam [125], seen **Figure 4H**. In 2018, O. Tsilipakos et al. used a magnetic dipole with a ring dipole

resonator in the metasurface unit made of an elliptical dielectric rod. When the rod dielectric constant is changed, the effect of accurately matching the two resonances can be achieved, realizing the manipulation of constructing a tunable gradient metasurface and reconfiguring its wave front [126], seen in **Figure 4I**.

This type of reconfigurable metasurface is voltage controlled and has the characteristics of simple tuning abilities. However, it is difficult to achieve on-demand independent control of each single metasurface unit for material-loaded metasurfaces discussed above. Therefore, there are no reports of metasurface applications with better functional performance. Fortunately, in view of the engineering feasibility of electronically controlled reconfigurable metasurface loaded by diodes, the researchers further proposed the idea of coding and reprogrammable metasurface designs. Quite recently, researchers from Southeast University in China have systematically studied the working principle as well as design method of digital coding metasurface and reprogrammable metasurface [99], as shown in **Figure 5A**. For example, in 2018, L. Zhang et al. proposed the concept of space-time modulated digital coding metasurface to achieve the simultaneous manipulation of electromagnetic wave frequency domain and space; thereby, harmonic beam control was achieved [127], as shown in **Figure 5B**. The design principle of the space-time digital coded metasurface can be applied to various aspects such as wireless

FIGURE 6 | Optically reconfigurable metasurface. **(A)** Loaded with phase change material [131], **(B)** loaded with additional silicon ring layer [132], **(C)** loaded with ion-implanted silicon layer [133], **(D)** loaded with specific dielectric materials [134], and **(E)** loaded with photodiodes [135].

communication and holographic imaging. Other functional devices such as reconfigurable holographic imaging metasurfaces with transformable multibeam radiation have also been developed [128] as shown in **Figure 5C**. Based on the breakthroughs obtained by the T. Cui's research group, the smart metasurface imager and recognizer empowered by a network of artificial neural network (ANNs) for the adaptive control data flow and the smart metasurface that has self-adaptive reprogrammable functions without human participation have been designed [129, 130], as shown in **Figures 5D and 5E**.

Optically Reconfigurable Metasurface

In recent years, researchers have also proposed to load photosensitive materials as well as devices into metasurface structures to achieve optically reconfigurable metasurface by adjusting the intensity of light sources. For examples, in 2016, Q. Wang et al. used a phase change material (chalcogenide GST) as the metasurface substrate material to realize a light-controlled dual-focus reconfigurable metasurface structure [131], seen in **Figure 6A**. In 2018, L. Cong et al. used a layer of silicon ring between a conventional C-shaped metasurface unit and a sapphire substrate, as shown in **Figure 6B**. By changing the intensity of the pump light, fast switching of the polarization state of the incident electromagnetic wave and rapid separation of the copolarized/cross-polarized wave were achieved [132]. In the same year, H. Cai et al. designed an ultrafast tunable metasurface consisting of an array of ion-implant combined with annealed silicon disk using optical pump terahertz probe

spectroscopy to perform ultrafast and efficient all-optical tuning of silicon-based metasurfaces, seen in **Figure 6C**, in turn, achieving ultra-fast effective all-optical modulation of THz waves [133].

In 2018, K. Fan et al. overcame the static geometric tuning characteristics of traditional dielectric metasurfaces, by controlling the resonant eigenmodes through optical excitation. The optically tunable characteristics of the dynamic dielectric Huygens' metasurface were proposed and verified, which has great significance for the application of metasurface reconfigurability, as shown in **Figure 6D** [134]. In addition, the T. Cui's group from Southeast University integrated the photodiode into the metasurface array to develop the light-controlled reconfigurable metasurface structure by digitally encoding the LED illumination state, as shown in **Figure 6F** [135]. However, the use of additional light sources to control the electromagnetic response characteristics of metasurface unit to achieve reconfigurable function increases the complexity as well as cost of the system to some extent.

Thermally Reconfigurable Metasurface

It is well known that some of the substrate materials described above such as silicon, liquid crystal, and phase change material GST are sensitive to bias voltage, light intensity, and also the background temperature. Based on the temperature sensitivity of these materials, researchers have proposed thermally reconfigurable metasurfaces in recent years. As can be seen in **Figures 7A** and **7B**, the Y. Kivshar's Group of the Australian National University has used silicon and liquid crystal as the
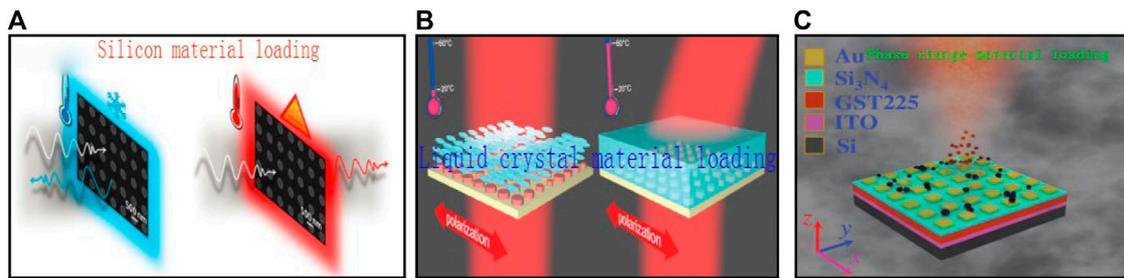
FIGURE 7 | Thermally reconfigurable metasurface. **(A)** Loaded with silicon [136], **(B)** loaded with liquid crystal [137], and **(C)** loaded with phase change material [140].
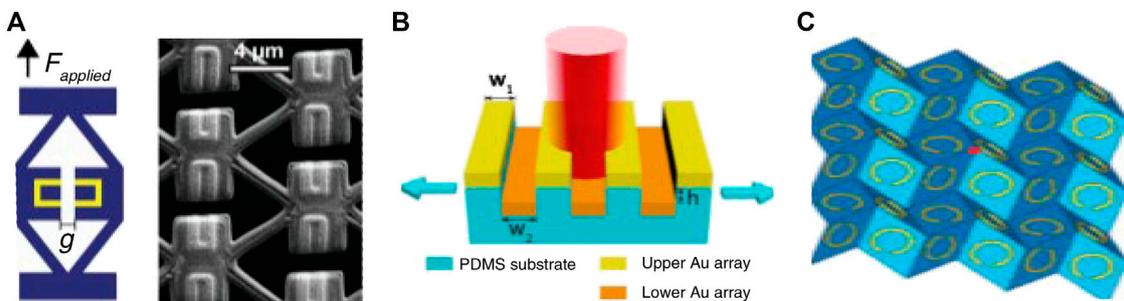
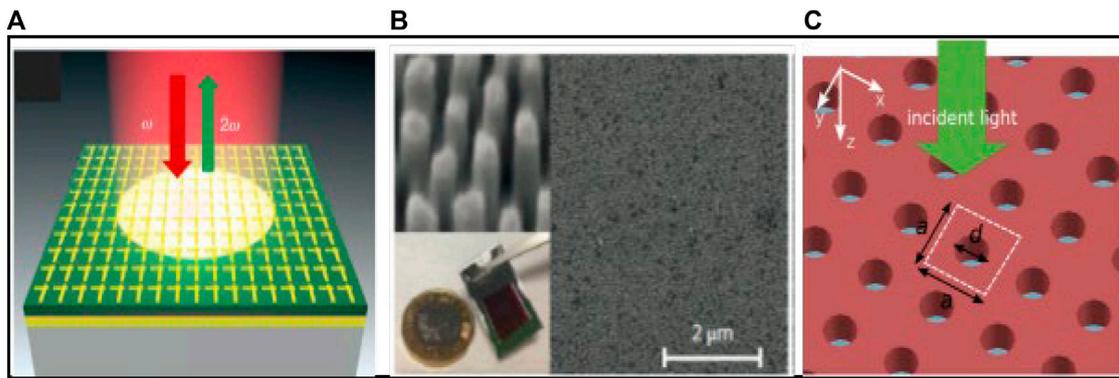**FIGURE 8 |** Mechanical reconfigurable metasurface [132–134].

substrate material of the metasurface. By adjusting the temperature around the metasurface, it can realize the dynamic control of the reflection/transmission of incident electromagnetic waves and dynamic control of the transmission direction of incident electromagnetic waves [136, 137]. W. Dong et al. achieved the adjustment of the transmitted electromagnetic wave operating band by using the temperature-sensitive phase-change material GST loaded into metasurface [138]. In 2018, H. Cai et al. proposed a vanadium dioxide-based hybrid metasurface and the hybrid metasurface can realize the control of transmission of terahertz waves by heating, or optical pumping [139]. In the same year, J. Tian et al. used a phase change material such as $Ge_2Sb_2Te_5$ (GST) to switch the material phase state between a crystal and an amorphous crystal by changing the temperature to switch the response of the meta-atom between an electric and a magnetic dipole. The phase shift generated by the multistage resonance realizes wave front manipulation. It will contribute to the development of future optical communication networks [140]. At the same time, X. Chen et al. used shape memory alloy as the metasurface substrate material and changed the shape of the memory alloy by adjusting the ambient temperature to develop a transmissive metasurface structure with tunable working frequency band [141]. The thermally reconfigurable metasurface provides a solution to a certain extent, but the prepared metasurface was greatly affected by

the environmental temperature changings. Aside from that, its practicability and operability are limited.

Mechanically Reconfigurable Metasurface

When the metasurface array was prepared on the elastic/flexible substrate material, the shape of the elastic/flexible substrate material can be mechanically adjusted. As a result, the electromagnetic response of the metasurface unit could also be changed, to achieve a mechanically reconfigurable metasurface. In 2018, J. Reeves et al. designed a metasurface as directed in **Figure 8A**. The C-shaped metasurface unit was prepared on a soft polymer scaffold by additional stretching/compression soft polymerization. The object holder can control the spacing of two C-shaped units in the metasurface unit to realize the mechanical reconfigurable metasurface structure [142]. X. Liu et al. also proposed a noncoplanar metasurface structure as shown in **Figure 8B**. The two-layer metasurface array was fabricated on a PDMS flexible substrate. The mechanically reconfigurable metasurface was achieved by stretching the PDMS flexible material to change the coupling characteristics between the two metasurface arrays [143].

In addition, Z. Wang et al. prepared a C-shaped metasurface unit on a foldable dielectric substrate as can be seen in **Figure 8C**. Different chiral responses to incident electromagnetic waves were achieved by changing the folding mode of the dielectric substrate [144]. L. Chen et al. changed the distance of the reflective surface

FIGURE 9 | Nonlinear metasurface and power reconfigurable metasurface [136–138].

of the metasurface metal reflective surface from the metasurface layer by mechanical means to realize the reconfigurable function of the reflected beam [145]. The mechanical reconfigurable metasurface provides a feasible solution for real-time dynamic control of electromagnetic waves. However, its mechanical control system is complex and it is difficult to achieve precise control with the high-performance metasurface applications.

Power Reconfigurable Metasurface

In addition, researchers have proposed the design idea of nonlinear metasurface to achieve the generation of higher harmonics and manipulation of its characteristics [100]. In 2014, J. Lee et al. developed an asymmetric cross-shaped unit and a metasurface array using the principle of electron complementary band transition in a semiconductor heterostructure. As a result, a second-order nonlinear harmonic output with high conversion efficiency was achieved [146] as shown in **Figure 9A**. In 2017, based on the relationship between electromagnetic response characteristics of the nonlinear metasurface and the incident electromagnetic wave intensity, L. Nicholls et al. designed a metasurface that can quickly adjust the polarization direction of the electromagnetic wave as shown in **Figure 9B**. The nonlinear metasurface was able to realize the polarization deflection of electromagnetic waves of up to 60° under the excitation of electromagnetic waves with different intensities [147]. In 2018, Y. Xu et al. used chalcogenide glass to prepare a full-dielectric metasurface as can be seen in **Figure 9C**. Based on the high nonlinearity of chalcogenide glass, the switching control of the vortex electromagnetic wave state was achieved by adjusting the incident electromagnetic wave intensity [148]. In 2018, L. Wang et al. proposed a nonlinear all-dielectric metasurface which generates a third harmonic signal and efficiently controls the nonlinear wave front of any complex parameter wave generated by it. Its control efficiency can reach up to 92% [149]. The nonlinear metasurface energy can realize the reconfigurable property of the electromagnetic wave self-control ability simply by adjusting the incident electromagnetic wave intensity. However, in the reported nonlinear metasurface, it is difficult to effectively control each single metasurface unit, so a more versatile reconfigurable metasurface structure is hard to be realized.

In recent years, optomechanical nonlinear metasurfaces [149–151] have received wide attention as a new class of nonlinear metasurfaces. The metal/nonmetal resonant unit in the optomechanical metasurface is prepared on the elastic material matrix or the resonant unit itself is suspended to form an elastic structure. Under the excitation of the incident electromagnetic wave, the field-structure interaction will generate optical gradient force, electromagnetic induction force, and/or thermal expansion force. The optomechanical metasurface can control the self-polarization state of incident electromagnetic waves by adjusting the intensity of incident electromagnetic waves [150, 151]. The nonlinear characteristics of optomechanical metasurfaces are derived from the mutual coupling effect of incident electromagnetic wave energy and metasurface unit structure potential energy.

DISCUSSION AND PERSPECTIVE

As can be seen above, the researches on electromagnetic metasurface have made remarkable progress in mechanism discovery, analytical theory breakthrough, application innovation, etc. In recent years, a variety of metasurface implementation methods have been proposed to design metasurfaces with various electromagnetic wave response characteristics to achieve the electromagnetic wave amplitude, phase, polarization direction/state, orbital angular momentum, and spin angular momentum control. Based on the metasurfaces breakthrough, a variety of novel planar function devices and systems with microwave, THz, and optical frequency bands have been developed. For the various metasurfaces, especially the active tunable/reconfigurable/programmable ones, some of them already realized to independently control each metasurface unit.

In the near future, the metasurface can be further widely developed, with more efficient [24, 31, 76, 97, 118], wider operating bandwidth [12, 42, 118, 119] and easier fabrication and lower cost [152, 153]. Most importantly, metasurface can be designed based the cutting-edge techniques, including the artificial intelligent, to achieve the intelligent metasurface and smart metasurface, which are proposed in the past two years

[129, 130, 154–157]. This should be the most exciting research area in the metasurface research community.

CONCLUSION

This review firstly discussed the previously well-developed electromagnetic metasurfaces, in terms of the different kinds of modulations, including the magnitude, phase, and/or polarization modulations. Then, based on the analysis of the aforementioned metasurfaces which cannot realize the dynamic control, the active/tunable/reconfigurable metasurfaces based on various materials/components loadings are analyzed, in terms of the different kinds of control methods, including the electrically, optically, thermally, mechanically, and power reconfigurable/control techniques. In the end, the cutting-edge metasurface design idea based on mechanical learning, deep learning, is pointed out. This review concluded the main research directions in the past several years and it has important value for the metasurface research community.

AUTHOR CONTRIBUTIONS

FUNDING

REFERENCES

1. Cui TJ, Smith DR, Liu R. *Metamaterials: theory, design and applications*. New York, NY: Spring-Verlag (2010).

2. Sakai O, Tachibana K. Plasmas as metamaterials: a review. *Plasma Sources Sci Technol* (2012) 21(1):013001. doi:10.1088/0963-0252/21/1/013001

3. Wang Z, Cheng F, Winsor T, Liu Y. Optical chiral metamaterials: a review of the fundamentals, fabrication methods and applications. *Nanotechnology* (2016) 27(41):412001. doi:10.1088/0957-4484/27/41/412001

4. Ren X, Das R, Tran P, Ngo TD, Xie YM, et al. Auxetic metamaterials and structures: a review. *Smart Materials Structures* (2018) 27(2):023001. doi:10.1088/1361-665X/aaa61c

5. Cummer SA, Christensen J, Alù A. Controlling sound with acoustic metamaterials. *Nat Rev Materials* (2016) 1(3):1–13. doi:10.1038/natrevmats.2016.1

6. Yu X, Zhou J, Liang H, Jiang Z, Wu L. Mechanical metamaterials associated with stiffness, rigidity and compressibility: a brief review. *Prog Mater Sci* (2018) 94:114–73. doi:10.1016/j.pmatsci.2017.12.003

7. Chen HT, Padilla WJ, Zide JM, Gossard AC, Taylor AJ, Averitt RD. Active terahertz metamaterial devices. *Nature* (2006) 444(7119):597–600. doi:10.1038/nature05343

8. Dong Y, Itoh T. Metamaterial-based antennas. *Proc IEEE* (2012) 100(7):2271–85. doi:10.1109/JPROC.2012.2187631

9. Oliveri G, Werner DH, Massa A. Reconfigurable electromagnetics through metamaterials: a review. *Proc IEEE* (2015) 103(7):1034–56. doi:10.1109/JPROC.2015.2394292

10. Huang Y, Wu Z, Li J, Lv W, Xie F, Wen G, et al. Dynamics analysis of a pair of ring resonators in liquid media. *Phys Rev Appl* (2018) 10:044026. doi:10.1103/PhysRevApplied.10.044026

11. Lv W, Xie F, Huang Y, Li J, Fang X, Rashid A, et al. Nonlinear coupling states study of electromagnetic force actuated plasmonic nonlinear metamaterials. *Optic Express* (2018) 26:3211–20. doi:10.1364/OE.26.003211

12. Yu P, Besteiro LV, Huang Y, Wu J, Fu L, Tan HH, et al. Broadband metamaterial absorbers. *Adv Opt Mater* (2019) 7:1800995. doi:10.1002/adom.201800995

13. Yu P, Besteiro LV, Wu J, Huang Y, Wang Y, Govorov AO, et al. Metamaterial perfect absorber with unabated size-independent absorption. *Optic Express* (2018) 26:20471–80. doi:10.1364/OE.26.020471

14. Huang Y, Wen G, Zhu W, Li J, Si LM, Premaratne M. Experimental demonstration of a magnetically tunable ferrite based metamaterial absorber. *Optic Express* (2014) 22:16408–17. doi:10.1364/OE.22.016408

15. Zhu W, Huang Y, Rukhlenko I, Wen G, Premaratne M. Configurable metamaterial absorber with pseudo wideband spectrum. *Optic Express* (2012) 20(6):6616–21. doi:10.1364/OE.20.006616

16. Li Y, Zhu KJ, Peng YG, Li W, Yang T, Xu HX, et al. Thermal meta-device in analogue of zero-index photonics. *Nat Mater* (2019) 18(1):48–54. doi:10.1038/s41563-018-0239-6

17. Luo X. Subwavelength optical engineering with metasurface waves. *Adv Opt Mater* (2018) 6:1701201. doi:10.1002/adom.201701201

18. Kildishev AV, Boltasseva A, Shalaev VM. Planar photonics with metasurfaces. *Science* (2013) 339(6125):1232009–6. doi:10.1126/science.1232009

19. Lin D, Fan P, Hasman E, Brongersma ML. Dielectric gradient metasurface optical elements. *Science* (2014) 345(6194):298–302. doi:10.1126/science.1253213

20. Holloway CL, Kuester EF, Gordon JA, O'Hara J, Booth J, Smith DR. An overview of the theory and applications of metasurfaces: the two-dimensional equivalents of metamaterials. *IEEE Antenn Propag Mag* (2012) 54(2):10–35. doi:10.1109/MAP.2012.6230714

21. Fan Y, Shen N, Zhang F, Zhao Q, Wei Z, Zhang P, et al. Photoexcited graphene metasurfaces: significantly enhanced and tunable magnetic resonances. *ACS Photon* (2018) 5(4):1612–1618. doi:10.1021/acsphotonics.8b00057

22. Huang Y, Yang L, Li J, Wang Y, Wen G. Polarization conversion of metasurface for the application of wide band low-profile circular polarization slot antenna. *Appl Phys Lett* (2016) 109:054101. doi:10.1063/1.4960198

23. Li Z, Premaratne M, Zhu W. Advanced encryption method realized by secret shared phase encoding scheme using a multi-wavelength metasurface. *Nanophotonics* (2020) 9:20200298. doi:10.1515/nanoph-2020-0298

24. Bai X, Kong F, Sun Y, Wang G, Qian J, Li X, et al. High-efficiency transmissive programmable metasurface for multimode OAM generation. *Adv Opt Mater* (2020) 8:202000570. doi:10.1002/adom.202000570

25. Akram MR, Ding G, Chen K, Feng Y, Zhu W. Ultrathin single layer metasurfaces with ultra-wideband operation for both transmission and reflection. *Adv Mater* (2020) 32(12):e1907308. doi:10.1002/adma.201907308

26. Hu G, Hong X, Wang K, Wu J, Xu HX, Zhao W, et al. Coherent steering of nonlinear chiral valley photons with a synthetic Au–WS 2 metasurface. *Nat Photon* (2019) 13(7):467–72. doi:10.1038/s41566-019-0399-1

27. Xu HX, Han L, Li Y, Sun Y, Zhao J, Zhang S, et al. Completely spin-decoupled dual-phase hybrid metasurfaces for arbitrary wavefront control. *ACS Photon* (2018) 6(1):211–20. doi:10.1021/acsphotonics.8b01439

28. Li C, Yu P, Huang Y, Zhou Q, Wu J, Li Z, et al. Dielectric metasurfaces: from wavefront shaping to quantum platforms. *Prog Surf Sci* (2020) 95(2):100584. doi:10.1016/j.progsurf.2020.100584

29. Huang Y, Li J, Xu HX, Yu H, Yang Z, Yu P, et al. Experimental demonstration of microwave two-dimensional Airy beam generation based on single-layer metasurface. *IEEE Trans Antenn Propag* (2020) 68(11):7507–16. doi:10.1109/TAP.2020.2996826

30. Xu HX, Hu G, Jiang M, Tang S, Wang Y, Wang C, et al. Wavevector and frequency multiplexing performed by a spin-decoupled multichannel metasurface. *Advan Mater Tech* (2020) 5(1):1900710. doi:10.1002/admt.201900710

31. Dai JY, Yang LX, Ke JC, Chen MZ, Tang W, Li X, et al. High-efficiency synthesizer for spatial waves based on space-time-coding digital metasurface. *Laser Photon Rev* (2020) 14(6):1900133. doi:10.1002/lpor.201900133

32. Li H, Li YB, Shen JL, Cui TJ. Low-profile electromagnetic holography by using coding fabry–perot type metasurface with in-plane feeding. *Advan Optical Mater* (2020) 8(9):1902057. doi:10.1002/adom.201902057

33. Zhang XG, Yu Q, Jiang WX, Sun YL, Bai L, Wang Q, et al. Polarization-controlled dual-programmable metasurfaces. *Advan Sci* (2020) 7(11):1903382. doi:10.1002/advs.201903382

34. Wu RY, Bao L, Wu LW, Wang Z, Ma Q, Wu JW, et al. Independent control of copolarized amplitude and phase responses via anisotropic metasurfaces. *Advan Optical Mater* (2020) 8(9):1902126. doi:10.1002/adom.201902126

35. Zhang XG, Jiang WX, Jiang HL, Wang Q, Tian H, Bai L, et al. An optically driven digital metasurface for programming electromagnetic functions. *Nat Electron* (2020) 3(3):165–71. doi:10.1038/s41928-020-0380-5

36. Yu N, Capasso F. Flat optics with designer metasurfaces. *Nat Mater* (2014) 13(2):139–50. doi:10.1038/nmat3839

37. Meinzer N, Barnes WL, Hooper IR (2014). Plasmonic meta-atoms and metasurfaces. *Nat Photon*. 8(12):889–98. doi:10.1038/nphoton.2014.247

38. Khorasaninejad M, Capasso F. Perfect anomalous reflection with a bipartite Huygens' metasurface. *Science* (2017) 358:eaam8100. doi:10.1126/science.aam8100

39. Wong AMH, Eleftheriades GV. Perfect anomalous reflection with a bipartite Huygens' metasurface. *Phys Rev X* (2018) 8(1):11036. doi:10.1103/PhysRevX.8.011036

40. Kamali SM, Arbabi E, Arbabi A, Faraon A. A review of dielectric optical metasurfaces for wavefront control. *Nanophotonics* (2018) 7(6):1041–68. doi:10.1515/nanoph-2017-0129

41. Nagarajan A, van Erve K, Gerini G. Ultra-narrowband polarization insensitive transmission filter using a coupled dielectric-metal metasurface. *Optic Express* (2020) 28(1):773–87. doi:10.1364/OE.383781

42. Sun D, Qi L, Liu Z. Terahertz broadband filter and electromagnetically induced transparency structure with complementary metasurface. *Results Phys* (2020) 16:102887. doi:10.1016/j.rinp.2019.102887

43. Zhang Z, Yang Q, Gong M, Chen M, Long Z. Metasurface lens with angular modulation for extended depth of focus imaging. *Opt Lett* (2020) 45(3):611–4. doi:10.1364/OL.382812

44. Sung J, Lee GY, Lee B. Progresses in the practical metasurface for holography and lens. *Nanophotonics* (2019) 8(10):1701–18. doi:10.1515/nanoph-2019-0203

45. Yuan Y, Zhang K, Ratni B, Song Q, Ding X, Wu Q, et al. Independent phase modulation for quadruplex polarization channels enabled by chirality-assisted geometric-phase metasurfaces. *Nat Commun* (2020) 11(1):4186–9. doi:10.1038/s41467-020-17773-6

46. Yuan Y, Sun S, Chen Y, Zhang K, Ding X, Ratni B, et al. A fully phase-modulated metasurface as an energy-controllable circular polarization router. *Adv Sci* (2020) 7(18):2001437. doi:10.1002/advs.202001437

47. Castaldi G, Zhang L, Moccia M, Hathaway AY, Tang W, Cui TJ, et al. Joint multi-frequency beam shaping and steering via space-time-coding digital metasurfaces. *Adv Funct Mater* (2020) 2020:2007620. doi:10.1002/adfm.202007620

48. Wei Q, Huang L, Zentgraf T, Wang Y. Optical wavefront shaping based on functional metasurfaces. *Nanophotonics* (2020) 9:478. doi:10.1515/nanoph-2019-0478

49. Ren H, Briere G, Fang X, Ni P, Sawant R, Héron S, et al. Metasurface orbital angular momentum holography. *Nat Commun* (2019) 10(1):2986–8. doi:10.1038/s41467-019-11030-1

50. Hermon S, Ma A, Yue F, Kubrom F, Intaravanne Y, Han J, et al. Metasurface hologram for polarization measurement. *Opt Lett* (2019) 44(18):4436–8. doi:10.1364/OL.44.004436

51. Hedayati MK, Elbahri M. Review of metasurface plasmonic structural color. *Plasmonics* (2017) 12(5):1463–79. doi:10.1007/s11468-016-0407-y

52. Imani MF, Gollub JN, Yurduseven O, Diebold AV, Boyarsky M, Fromenteze T, et al. Review of metasurface antennas for computational microwave imaging. *IEEE Trans Antenn Propag* (2020) 68(3):1860–75. doi:10.1109/TAP.2020.2968795

53. Amer AAG, Sapuan SZ, Nasimuddin N, Alphones A, Zinal NB. A comprehensive review of metasurface structures suitable for RF energy harvesting. *IEEE Access* (2020) 8:76433–52. doi:10.1109/ACCESS.2020.2989516

54. Bukhari SS, Vardaxoglou JY, Whittow W. A metasurfaces review: definitions and applications. *Appl Sci* (2019) 9(13):2727. doi:10.3390/app9132727

55. Ding F, Bozhevolnyi SI. A review of unidirectional surface plasmon polariton metacouplers. *IEEE J Sel Top Quant Electron* (2019) 25(3):1–11. doi:10.1109/JSTQE.2019.2894067

56. Ding F, Pors A, Bozhevolnyi SI. Gradient metasurfaces: a review of fundamentals and applications. *Rep Prog Phys* (2017) 81(2):026401. doi:10.1088/1361-6633/aa8732

57. Ding F, Yang Y, Deshpande RA, Bozhevolnyi SI. A review of gap-surface plasmon metasurfaces: fundamentals and applications. *Nanophotonics* (2018) 7(6):1129–56. doi:10.1515/nanoph-2017-0125

58. Hu J, Bandyopadhyay S, Liu Y. A review on metasurface: from principle to smart metadevices. *Front Phys* (2020) 8:502. doi:10.3389/fphy.2020.586087

59. Chen HT, Taylor AJ, Yu N. A review of metasurfaces: physics and applications. *Rep Prog Phys* (2016) 79(7):076401. doi:10.1088/0034-4885/79/7/076401

60. Deng ZL, Li G. Metasurface optical holography. *Mater Today Phys* (2017) 3:16–32. doi:10.1016/j.mtphys.2017.11.001

61. Arbabi A, Horie Y, Bagheri M, Faraon A. Dielectric metasurfaces for complete control of phase and polarization with subwavelength spatial resolution and high transmission. *Nat Nanotechnol* (2015) 10(11):937–43. doi:10.1038/nnano.2015.186

62. Shaltout AM, Kinsey N, Kim J, Chandrasekar R, Ndukaife JC, Boltasseva A, et al. Development of optical metasurfaces: emerging concepts and new materials. *Proc IEEE* (2016) 104(12):2270–87. doi:10.1109/JPROC.2016.2590882

63. Akselrod GM, Huang J, Hoang TB, Bowen PT, Su L, Smith DR, et al. Large-area metasurface perfect absorbers from visible to near-infrared. *Adv Mater Weinheim* (2015) 27(48):8028–34. doi:10.1002/adma.201503281

64. Horie Y, Arbabi A, Arbabi E, Kamali SM, Faraon A. Wide bandwidth and high resolution planar filter array based on DBR-metasurface-DBR structures. *Optic Exp* 24 (2016) 11677–82. doi:10.1364/OE.24.011677

65. Sun H, Wen G, Huang Y, Li J, Zhu W, Si LM. Tunable band notch filters by manipulating couplings of split ring resonators. *Appl Optic* (2013) 52(31):7517–22. doi:10.1364/AO.52.007517

66. Li Z, Wang W, Rosenmann D, Czaplewski DA, Yang X, Gao J. All-metal structural color printing based on aluminum plasmonic metasurfaces. *Optic Exp* (2016) 24(18):20472. doi:10.1364/OE.24.020472

67. Kim TT, Kim H, Kenney M, Park HS, Kim HD, Min B, et al. Amplitude modulation of anomalously refracted terahertz waves with gated-graphene

metasurfaces. *Adv Opt Mater* (2018) 6(1):201700507. doi:10.1002/adom. 201700507

68. Song X, Huang L, Tang C, Li J, Li X, Liu J, et al. Selective diffraction with complex amplitude modulation by dielectric metasurfaces. *Adv Opt Mater* (2018) 6(4):1701181. doi:10.1002/adom.201701181

69. Song X, Huang L, Sun L, Zhang X, Zhao R, Li X, et al. Near-field plasmonic beam engineering with complex amplitude modulation based on metasurface. *Appl Phys Lett* (2018) 112:73104. doi:10.1063/1.5013327

70. Yu N, Genevet P, Kats MA, Aieta F, Tetienne JP, Capasso F, et al. Light propagation with phase discontinuities: generalized laws of reflection and refraction. *Science* (2011) 334(6054):333–7. doi:10.1126/science.1210713

71. Aieta F, Genevet P, Kats MA, Yu N, Blanchard R, Gaburro Z, et al. Aberration-free ultrathin flat lenses and axicons at telecom wavelengths based on plasmonic metasurfaces. *Nano Lett* (2012) 12(9):4932–6. doi:10.1021/nl302516v

72. Zhang L, Mei S, Huang K, Qiu CW. Advances in full control of electromagnetic waves with metasurfaces. *Adv Opt Mater* (2016) 4(6):818–33. doi:10.1002/adom.201500690

73. Ding X, Monticone F, Zhang K, Zhang L, Gao D, Burokur SN, et al. Ultrathin pancharatnam-berry metasurface with maximal cross-polarization efficiency. *Adv Mater Weinheim* (2015) 27(7):1195–200. doi:10.1002/adma.201405047

74. Wen D, Yue F, Li G, Zheng G, Chan K, Chen S, et al. Helicity multiplexed broadband metasurface holograms. *Nat Commun*, 6 (2015)(6) 8241–7. doi:10.1038/ncomms9241

75. Maguid E, Chriki R, Yannai M, Kleiner V, Hasman E, Friesem AA, et al. Topologically controlled intracavity laser modes based on pancharatnam-berry phase. *ACS Photon* (2018) 5(5):1817–21. doi:10.1021/acsphotonics. 7b01525

76. Luo W, Sun S, Xu HX, He Q, Zhou L. Transmissive ultrathin pancharatnam-berry metasurfaces with nearly 100% efficiency. *Phys Rev Appl* (2017) 7(4): 44033. doi:10.1103/PhysRevApplied.7.044033

77. Li J, Yao J. Manipulation of terahertz wave using coding pancharatnam-berry phase metasurface. *IEEE Photonics J* (2018) 10:5900512. doi:10.1109/JPHOT. 2018.2866490

78. Zheng G, Mühlenbernd H, Kenney M, Li G, Zentgraf T, Zhang S. Metasurface holograms reaching 80% efficiency. *Nat Nanotechnol* (2015) 10(4):308–12. doi:10.1038/nnano.2015.2

79. Pfeiffer C, Grbic A. Metamaterial Huygens' surfaces: tailoring wave fronts with reflectionless sheets. *Phys Rev Lett* (2013) 110(19):197401–5. doi:10.1103/PhysRevLett.110.197401

80. Pfeiffer C, Boltasseva A. Efficient light bending with isotropic metamaterial Huygens' surfaces. *Nano Lett* (2014) 14:2491–7. doi:10.1021/nl5001746

81. Wang L, Kruk S, Tang H, Li T, Kravchenko I, Neshev DN, et al. Grayscale transparent metasurface holograms. *Optica* (2016) 3(12):1504. doi:10.1364/OPTICA.3.001504

82. Wang Z, Ding X, Zhang K, Ratni B, Burokur SN, Gu X, et al. Huygens metasurface holograms with the modulation of focal energy distribution. *Adv Opt Mater* (2018) 6:1800121. doi:10.1002/adom.201800121

83. Qin F, Ding L, Zhang L, Monticone F, Chum CC, Deng J, et al. Hybrid bilayer plasmonic metasurface efficiently manipulates visible light. *Sci Adv* (2016) 2: e1501168. doi:10.1126/sciadv.1501168

84. Arbabi A, Arbabi E, Horie Y, Kamali SM, Faraon A. Planar metasurface retroreflector. *Nat Photon* (2017) 11(7):415–20. doi:10.1038/nphoton. 2017.96

85. Wu C, Arju N, Kelp G, Fan J, Dominguez J, Gonzales E, et al. Spectrally selective chiral silicon metasurfaces based on infrared Fano resonances. *Nat Commun* (2014) 5:3892. doi:10.1038/ncomms4892

86. Pfeiffer C, Zhang C, Ray V, Guo LJ, Grbic A. High performance bianisotropic metasurfaces: asymmetric transmission of light. *Phys Rev Lett* (2014) 113(2): 023902–5. doi:10.1103/PhysRevLett.113.023902

87. Pfeiffer C, Zhang C, Ray V, Guo LJ, Grbic A. Polarization rotation with ultra-thin bianisotropic metasurfaces. *Optica* (2016) 3(4):427–32. doi:10.1364/OPTICA.3.000427

88. Balthasar Mueller JP, Rubin NA, Devlin RC, Groever B, Capasso F. Metasurface polarization optics: independent phase control of arbitrary orthogonal states of polarization. *Phys Rev Lett* (2017) 118(11):113901–5. doi:10.1103/PhysRevLett.118.113901

89. Huang X, Chen J, Yang H. High-efficiency wideband reflection polarization conversion metasurface for circularly polarized waves. *J Appl Phys* (2017) 122(4):043102. doi:10.1063/1.4996643

90. Yang W, Meng Q, Che W, Gu L, Xue Q. Low-profile wideband dual-circularly polarized metasurface antenna array with large beamwidth. *IEEE Antenn Wireless Propag Lett* (2018) 17(9):1613–6. doi:10.1109/LAWP.2018.2857625

91. Liu L, Zhang X, Kenney M, Su X, Xu N, Ouyang C, et al. Broadband metasurfaces with simultaneous control of phase and amplitude. *Adv Mater Weinheim* (2014) 26(29):5031–6. doi:10.1002/adma.201401484

92. Li Z, Cheng H, Liu Z, Chen S, Tian J. Plasmonic airy beam generation by both phase and amplitude modulation with metasurfaces. *Adv Opt Mater* (2016) 4(8):1230–5. doi:10.1002/adom.201600108

93. Song EY, Lee GY, Park H, Lee K, Kim J, Hong J, et al. Compact generation of airy beams with C-aperture metasurface. *Adv Opt Mater* (2017) 5(10):1601028. doi:10.1002/adom.201601028

94. Lee GY, Yoon G, Lee SY, Yun H, Cho J, Lee K, et al. Complete amplitude and phase control of light using broadband holographic metasurfaces. *Nanoscale* (2018) 10(9):4237–45. doi:10.1039/c7nr07154j

95. Li J, Chen S, Yang H, Li J, Yu P, Cheng H, et al. simultaneous control of light polarization and phase distributions using plasmonic metasurfaces. *Adv Func Mater* (2015) 25(5):704–10. doi:10.1002/adfm.201403669

96. Zhou Y, Cao X, Gao J, Yang H, Li S. Reconfigurable metasurface for multiple functions: magnitude, polarization and phase modulation. *Optic Express* (2018) 26(22):29451–9. doi:10.1364/OE.26.029451

97. Xu HX, Hu G, Lei H, Jiang M, Huang Y, Li Y, et al. Chirality-Assisted high-efficiency metasurfaces with independent control of phase, amplitude, and polarization. *Adv Opt Mater* (2018) 7:1801479. doi:10.1002/adom.201801479

98. Shaltout AM, Kildishev AV, Shalaev VM. Evolution of photonic metasurfaces: from static to dynamic. *J Opt Soc Am B* (2016) 33(3):501. doi:10.1364/JOSAB. 33.000501

99. Liu S, Cui TJ. Concepts, working principles, and applications of coding and programmable metamaterials. *Adv Opt Mater* (2017) 5(22):1700624. doi:10. 1002/adom.201700624

100. Krasnok A, Tymchenko M, Alù A. Nonlinear metasurfaces: a paradigm shift in nonlinear optics. *Mater Today* (2018) 21(1):8–21. doi:10.1016/j.mattod. 2017.06.007

101. Kafaie Shirmanesh G, Sokhoyan R, Pala RA, Atwater HA. Dual-gated active metasurface at 1550 nm with wide (>300°) phase tunability. *Nano Lett* (2018) 18(5):2957–63. doi:10.1021/acs.nanolett.8b00351

102. Nemati A, Wang Q, Hong M, Teng J. Tunable and reconfigurable metasurfaces and metadevices. *Opto-Electronic Adv* (2018) 1(5): 18000901–25. doi:10.29026/oea.2018.180009

103. Liu F, Pitilakis A, Mirmoosa MS, Tsilipakos O, Wang X, Tasolamprou AC, et al. Programmable metasurfaces: state of the art and prospects. In: 2018 IEEE International Symposium on Circuits and Systems (ISCAS); 2018 May 27–30; Florence, Italy. New York, NY: IEEE (2018). p. 1–5.

104. Chen K, Feng Y, Monticone F, Zhao J, Zhu B, Jiang T, et al. A reconfigurable active Huygens' metalens (2017). Available at: https://arxiv.org/abs/1702. 01920.

105. Li A, Kim S, Luo Y, Li Y, Long J, Sievenpiper DF. High-power transistor-based tunable and switchable metasurface absorber. *IEEE Trans Microw Theor Tech* (2017) 65(8):2810–8. doi:10.1109/TMTT.2017.2681650

106. Zhao X, Schalch J, Zhang J, Seren H, Duan G, Averitt R, et al. Electromechanically tunable metasurface transmission waveplate at terahertz frequencies. *Optica* (2018) 5:303–10. doi:10.1364/OPTICA.5. 000303

107. Arbabi E, Arbabi A, Kamali SM, Horie Y, Faraji-Dana M, Faraon A. MEMS-tunable dielectric metasurface lens. *Nat Commun* (2018) 9, 812. doi:10.1038/s41467-018-03155-6

108. Manjappa M, Pitchappa P, Singh N, Wang N, Zheludev NI, Lee C, et al. Reconfigurable MEMS Fano metasurfaces with multiple-input-output states for logic operations at terahertz frequencies. *Nat Commun* (2018) 9(1): 4056–10. doi:10.1038/s41467-018-06360-5

109. Biswas SR, Gutiérrez CE, Nemilentsau A, Lee IH, Oh SH, Avouris P, et al. Tunable graphene metasurface reflectarray for cloaking, illusion, and focusing. *Phys Rev Appl* (2018) 9(3):34021. doi:10.1103/PhysRevApplied.9. 034021

110. Komar A, Fang Z, Bohn J, Sautter J, Decker M, Miroshnichenko A, et al. Electrically tunable all-dielectric optical metasurfaces based on liquid crystals. *Appl Phys Lett* (2017) 110(7):071109. doi:10.1063/1.4976504

111. Xiao D, Liu YJ, Yin S, Liu J, Ji W, Wang B, et al. Liquid-crystal-loaded chiral metasurfaces for reconfigurable multiband spin-selective light absorption. *Optic Express* (2018) 26(19):25305–14. doi:10.1364/OE.26.025305

112. Yurduseven O, Marks D, Fromenteze T, Smith D. Dynamically reconfigurable holographic metasurface aperture for a mills-cross monochromatic microwave camera. *Optic Express* (2018) 26:5281–91. doi:10.1364/OE.26.005281

113. Gao X, Yang WL, Ma HF, Cheng Q, Yu XH, Cui TJ, et al. A reconfigurable broadband polarization converter based on an active metasurface. *IEEE Trans Antenn Propag* (2018) 66:6086–95. doi:10.1109/TAP.2018.2866636

114. Chen L, Ma HL, Ruan Y, Cui HY. Dual-manipulation on wave-front based on reconfigurable water-based metasurface integrated with PIN diodes. *J Appl Phys* (2019) 125(2):23107. doi:10.1063/1.5078660

115. Zhang J, Wei X, Rukhlenko ID, Chen HT, Zhu W. Electrically tunable metasurface with independent frequency and amplitude modulations. *ACS Photon* (2019) 7(1):265–71. doi:10.1021/acsphotonics.9b01532

116. Han S, Kim S, Kim S, Low T, Brar VW, Jang MS. Complete complex amplitude modulation with electronically tunable graphene plasmonic metamolecules. *ACS Nano* (2020) 14(1):1166–75. doi:10.1021/acsnano.9b09277

117. Chen D, Yang J, Huang J, Bai W, Zhang J, Zhang Z, et al. The novel graphene metasurfaces based on split-ring resonators for tunable polarization switching and beam steering at terahertz frequencies. *Carbon* (2019) 154: 350–6. doi:10.1016/j.carbon.2019.08.020

118. Quader S, Zhang J, Akram MR, Zhu W. Graphene-based high-efficiency broadband tunable linear-to-circular polarization converter for terahertz waves. *IEEE J Sel Top Quant Electron* (2020) 26(5):1–8. doi:10.1109/ JSTQE.2020.2969566

119. Zhang J, Wei X, Premaratne M, Zhu W. Experimental demonstration of an electrically tunable broadband coherent perfect absorber based on a graphene–electrolyte–graphene sandwich structure. *Photon Res* (2019) 7(8):868–74. doi:10.1364/PRJ.7.000868

120. Chen X, Tian Z, Lu Y, Xu Y, Zhang X, Ouyang C, et al. Electrically tunable perfect terahertz absorber based on a graphene salisbury screen hybrid metasurface. *Advan Optical Mater* (2020) 8(3):1900660. doi:10.1002/adom. 201900660

121. Islam MS, Sultana J, Biabanifard M, Vafapour Z, Nine MJ, Dinovitser A, et al. Tunable localized surface plasmon graphene metasurface for multiband superabsorption and terahertz sensing. *Carbon* (2020) 158:559–67. doi:10. 1016/j.carbon.2019.11.026

122. Yuan Y, Sun S, Chen Y, Zhang K, Ding X, Ratni B, et al. A fully phase-modulated metasurface as an energy-controllable circular polarization router. *Adv Sci* (2020) 7(18):2001437. doi:10.1002/advs.202001437

123. Chen H, Lu WB, Liu ZG, Geng MY (2020). Microwave programmable graphene metasurface. *ACS Photonics*. 7, 1425–35. doi:10.1021/ acsphotonics.9b01807

124. Hosseininejad SE, Rouhi K, Neshat M, Faraji-Dana R, Cabellos-Aparicio A, Abadal S, et al. Reprogrammable graphene-based metasurface mirror with adaptive focal point for THz imaging. *Sci Rep* (2019) 9(1):2868–9. doi:10. 1038/s41598-019-39266-3

125. Howes A, Wang W, Kravchenko I, Valentine J (2018). Dynamic transmission control based on all-dielectric Huygens metasurfaces. *Optica* 5(7):787–92. doi:10.1364/OPTICA.5.000787

126. Tsilipakos O, Tasolamprou A, Koschny T, Kafesaki M, Economou E, Soukoulis C. Pairing toroidal and magnetic dipole resonances in elliptic dielectric rod metasurfaces for reconfigurable wavefront manipulation in reflection. *Adv Opt Mater* (2018) 6:1800633. doi:10.1002/adom.201800633

127. Zhang L, Chen XQ, Liu S, Zhang Q, Zhao J, Dai JY, et al. Space-time-coding digital metasurfaces. *Nat Commun* (2018) 9:4334. doi:10.1038/s41467-018-06802-0

128. Li L, Jun Cui T, Ji W, Liu S, Ding J, Wan X, et al. Electromagnetic reprogrammable coding-metasurface holograms. *Nat Commun* (2017) 8, 197. doi:10.1038/s41467-017-00164-9

129. Li L, Shuang Y, Ma Q, Li H, Zhao H, Wei M, et al. Intelligent metasurface imager and recognizer. *Light Sci Appl* (2019) 8(1):97. doi:10.1038/s41377-019-0209-z

130. Ma Q, Bai GD, Jing HB, Yang C, Li L, Cui TJ. Smart metasurface with self-adaptively reprogrammable functions. *Light Sci Appl* (2019) 8(1):98. doi:10. 1038/s41377-019-0205-3

131. Wang Q, Rogers ETF, Gholipour B, Wang CM, Yuan G, Teng J, et al. Optically reconfigurable metasurfaces and photonic devices based on phase change materials. *Nat Photon* (2016) 10(1):60–5. doi:10.1038/nphoton. 2015.247

132. Cong L, Srivastava YK, Zhang H, Zhang X, Han J, Singh R. All-optical active THz metasurfaces for ultrafast polarization switching and dynamic beam splitting. *Light Sci Appl* (2018) 7(1):28. doi:10.1038/s41377-018-0024-y

133. Cai H, Huang Q, Hu X, Liu Y, Fu Z, Zhao Y, et al. All-optical and ultrafast tuning of terahertz plasmonic metasurfaces. *Adv Opt Mater* (2018) 6: 1800143. doi:10.1002/adom.201800143

134. Fan K, Zhang J, Liu X, Zhang GF, Averitt RD, Padilla WJ. Phototunable dielectric Huygens' metasurfaces. *Adv Mater* (2018) 30(22):1800278. doi:10. 1002/adma.201800278

135. Zhang XG, Tang WX, Jiang WX, Bai GD, Tang J, Bai L, et al. Light-controllable digital coding metasurfaces. *Adv Sci* (2018) 5(11):1801028. doi:10.1002/advs.201801028

136. Rahmani M, Xu L, Miroshnichenko AE, Komar A, Camacho-Morales R, Chen H, et al. Reversible thermal tuning of all-dielectric metasurfaces. *Adv Funct Mater* (2017) 27(31):1700580. doi:10.1002/adfm.201700580

137. Komar A, Paniagua-Domínguez R, Miroshnichenko A, Yu YF, Kivshar YS, Kuznetsov AI, et al. Dynamic beam switching by liquid crystal tunable dielectric metasurfaces. *ACS Photon* (2018) 5(5):1742–8. doi:10.1021/ acsphotonics.7b01343

138. Dong W, Qiu Y, Zhou X, Banas A, Banas K, Breese M, et al. Tunable mid-infrared phase-change metasurface. *Adv Opt Mater* (2017) 6:201701346. doi:10.1002/adom.201701346

139. Cai H, Chen S, Zou C, Huang Q, Liu Y, Hu X, et al. Multifunctional hybrid metasurfaces for dynamic tuning of terahertz waves. *Adv Opt Mater* (2018) 6(14):1800257. doi:10.1002/adom.201800257

140. Tian J, Li Q, Lu J, Qiu M. Reconfigurable all-dielectric antenna-based metasurface driven by multipolar resonances. *Optic Express* (2018) 26(18): 23918–25. doi:10.1364/OE.26.023918

141. Chen X, Gao J, Kang B. Achieving a tunable metasurface based on a structurally reconfigurable array using SMA. *Optic Express* (2018) 26(4): 4300–8. doi:10.1364/OE.26.004300

142. Reeves JB, Jayne RK, Stark TJ, Barrett LK, White AE, Bishop DJ. Tunable infrared metasurface on a soft polymer scaffold. *Nano Lett* (2018) 18(5): 2802–6. doi:10.1021/acs.nanolett.7b05042

143. Liu X, Huang Z, Zhu C, Wang L, Zang J. Out-of-Plane designed soft metasurface for tunable surface plasmon polariton. *Nano Lett* (2018) 18(2):1435–41. doi:10.1021/acs.nanolett.7b05190

144. Wang Z, Jing L, Yao K, Yang Y, Zheng B, Soukoulis CM, et al. Origami-based reconfigurable metamaterials for tunable chirality. *Adv Mater* (2017) 29(27): 1–7. doi:10.1002/adma.201700412

145. Chen L, Ma HL, Cui HY. Wavefront manipulation based on mechanically reconfigurable coding metasurface. *J Appl Phys* (2018) 124(4):43101. doi:10. 1063/1.5039679

146. Lee J, Tymchenko M, Argyropoulos C, Chen PY, Lu F, Demmerle F, et al. Giant nonlinear response from plasmonic metasurfaces coupled to intersubband transitions. *Nature* (2014) 511(7507):65–9. doi:10.1038/ nature13455

147. Nicholls LH, Rodríguez-Fortuño FJ, Nasir ME, Córdova-Castro RM, Olivier N, Wurtz GA, et al. Ultrafast synthesis and switching of light polarization in nonlinear anisotropic metamaterials. *Nat Photon* (2017) 11(10):628–33. doi:10.1038/s41566-017-0002-6

148. Xu Y, Sun J, Frantz J, Shalaev MI, Walasik W, Pandey A, et al. Reconfiguring structured light beams using nonlinear metasurfaces. *Optic Express* (2018) 26(23):30930–43. doi:10.1364/OE.26.030930

149. Zhu H, Yi F, Cubukcu E. Plasmonic metamaterial absorber for broadband manipulation of mechanical resonances. *Nat Photon* (2016) 10(11):709–14. doi:10.1038/nphoton.2016.183

150. Ou JY, Plum E, Zhang J, Zheludev NI. Giant nonlinearity of an optically reconfigurable plasmonic metamaterial. *Adv Mater Weinheim* (2016) 28(4): 729–33. doi:10.1002/adma.201504467

151. Zanotto S, Tredicucci A, Navarro-Urrios D, Cecchini M, Biasiol G, Mencarelli D, et al. Optomechanics of chiral dielectric metasurfaces. *Adv Opt Mater* (2019) 8(4):1901507. doi:10.1002/adom.201901507

152. Zhang M, Ma X, Pu M, Liu K, Guo Y, Huang Y, et al. Large-area and low-cost nanoslit-based flexible metasurfaces for multispectral electromagnetic wave manipulation. *Adv Optical Mater* (2019) 7(23):1900657. doi:10.1002/adom. 201900657

153. Long Z, Liang Y, Feng L, Zhang H, Liu M, Xu T. Low-cost and high sensitivity glucose sandwich detection using a plasmonic nanodisk metasurface. *Nanoscale* (2020) 12(19):10809–15. doi:10.1039/ d0nr00288g

154. Tang W, Chen MZ, Dai JY, Zeng Y, Zhao X, Jin S, et al. Wireless communications with programmable metasurface: new paradigms, opportunities, and challenges on transceiver design. *IEEE Wireless Commun* (2020) 27(2):180–7. doi:10.1109/MWC.001.1900308

155. Li L, Ruan H, Liu C, Li Y, Shuang Y, Alù A, et al. Machine-learning reprogrammable metasurface imager. *Nat Commun* (2019) 10(1):1082–8. doi:10.1038/s41467-019-09103-2

156. Qian C, Zheng B, Shen Y, Li J, Li E, Shen H, et al. Deep-learning-enabled self-adaptive microwave cloak without human intervention. *Nat Photon* (2020) 14(6):383–90. doi:10.1038/s41566-020-0604-2

157. Qian C, Lin X, Lin X, Xu J, Sun Y, Li E, et al. Performing optical logic operations by a diffractive neural network. *Light Sci Appl* (2020) 9(1):59. doi:10.1038/s41377-020-0303-2